Simplified model for calculating the pressure dependence of a direct current planar magnetron discharge

G. Buyle,[a] D. Depla, K. Eufinger, J. Haemers, and R. De Gryse
Department of Solid State Sciences, Ghent University, Krijgslaan 281 S1, B-9000 Ghent, Belgium

W. De Bosscher
Bekaert Advanced Coatings, E3-Laan 75/79, B-9800 Deinze, Belgium

(Received 17 October 2002; accepted 10 March 2003; published 1 July 2003)

A simplified model for the direct current planar magnetron discharge allowing one to simulate the pressure dependence over a wide range is presented. For sufficiently strong magnetic fields, the high energy electrons (HEE), the electrons that are responsible for the ionization, move predominantly in arch shaped regions in between interactions with the discharge gas. This allows one to model the discharge as being built up by arches. The influence of the interactions of the HEE on their motion is modeled by calculating the probabilities for transfer of HEE among the arch shaped regions. In this way the ionization distribution of the electrons emitted at a certain position at the target surface can be calculated. The results of this approach agree well with Monte Carlo results. This modeling of the HEE motion combined with simple schemes for determining the ionization and target erosion forms the core of the simplified model. The model is made self-consistent through iteration. It appears that for a given magnet system and discharge voltage a self-consistent solution is only possible for one particular pressure. This is the pressure for which the discharge voltage corresponds with the theoretical minimum discharge voltage needed to sustain the discharge at that pressure. The model reproduces the experimentally observed increase of the discharge voltage and widening of the erosion profile with decreasing pressure. According to the model the main cause for this pressure dependence is not the decreased confinement of electrons in the magnetic trap but the increased recapture of secondary electrons by the target. © *2003 American Vacuum Society.*
[DOI: 10.1116/1.1572169]

I. INTRODUCTION

The importance of magnetron sputtering as a deposition technique has made it the subject of numerous modeling and simulation efforts.[1] Our aim is to develop a model that gives insight into the discharge and that not only reproduces but also explains the experimentally observed influences of different external parameters on the discharge properties. Therefore, in spite of some loss of accuracy, the different processes occurring in the discharge have been separated and simplified in order to model them.

The electrons in the magnetron discharge can be divided in two groups: the ones with energy below the threshold energy for ionization $E_{\mathrm{ion,th}}$, and the ones with energies above $E_{\mathrm{ion,th}}$. In our model we will take into account only the latter and will refer to them as high energy electrons (HEE). The HEE originate from the target where they are released as secondary electrons (SE) or from the creation of an electron-ion pair in the cathode sheath. The amount of SE created per incoming ion is given by the SE yield γ. This yield can be considered as energy independent for the ion energies encountered in a magnetron discharge. A typical value is $\gamma=0.1$ for clean metal surfaces.[2] For a sufficiently strong magnetic field, the HEE move in arch shaped orbits because of their gyrating around the magnetic field lines.[3] Hence, the discharge can be considered as built up by arch shaped regions.[4]

[a]Electronic mail: guy.buyle@rug.ac.be

In this article we develop a model based on this consideration (Sec. II). In Sec. III results for the ionization distribution obtained by Monte Carlo (MC) simulations and by our approach are compared. Section IV discusses the results of our model for a given configuration and for the pressure dependence of the planar magnetron discharge.

II. MODEL

For a rectangular magnetron with two long straight sections that do not influence each other, the symmetric two-dimensional geometry shown in Fig. 1 is sufficient for modeling the discharge in these straight sections.[5] The magnet system is characterized by the strength of the magnets B_r, the spacing d between the centers of the magnets and the side length s of the square shaped magnets. The discharge is considered as being built up by arches A_i that correspond with positions x_i at regular distances along the x axis (Fig. 1). By introducing the arches A_i the HEE distribution H of the discharge is characterized by the occupation profile u that consists of a set of values u_i that give for each arch A_i its relative weight in the discharge

$$H=\sum_i u_i A_i . \tag{1}$$

Figure 1 represents an idealized situation because it is assumed that the arches are concentric circle segments which is

Downloaded 27 Dec 2012 to 152.14.136.96. Redistribution subject to AVS license or copyright; see http://avspublications.org/jvsta/about/rights_and_permissions

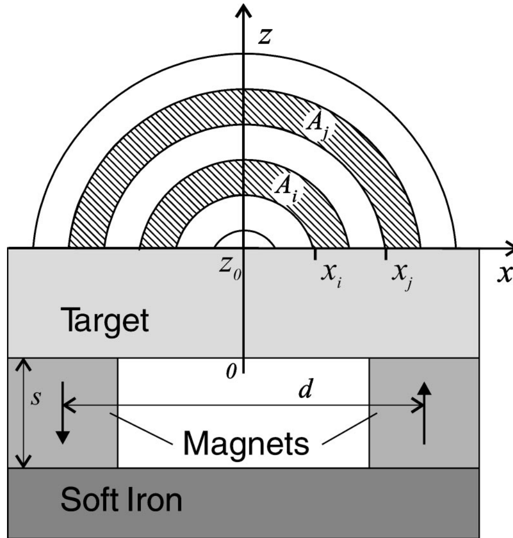

FIG. 1. Two-dimensional sketch of the magnetron model: the magnet system is defined by the side length s of the square shaped magnets, the distance d between the center of the magnets, the magnet strength B_r, and the target thickness z_0. The semicircles above the target indicate the idealized situation of how the discharge is built up.

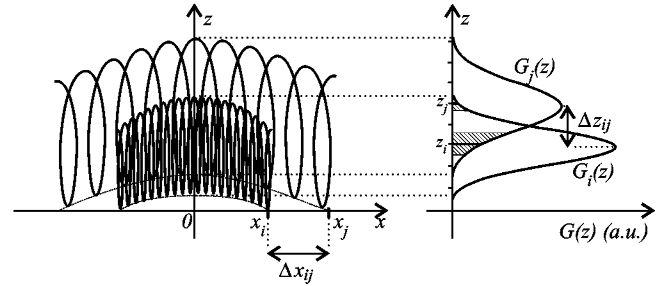

FIG. 2. For two positions x_i and x_j at the target surface, the position of the corresponding arches A_i and A_j are indicated by sketching the collisionless orbits of the SE emitted at these positions. The right-hand part shows the gaussian distributions attributed to the arches A_i and A_j. The transfer probability t_{ij} is proportional with the hatched surface under the gaussian G_j at z_i. Similarly, t_{ji} is determined by $G_i(z_j)$.

not the case for a realistic magnetic configuration. Hence, the first part of the model is to calculate the realistic arches and the electron distribution within.

A. Determination of the arches A_i

To determine the arch A_i the corresponding collisionless SE orbit with starting position x_i is calculated using the Lorentz equation

$$\frac{d\bar{v}}{dt}=\frac{q}{m}(\bar{E}+\bar{v}\times\bar{B}), \tag{2}$$

with q, m, $\bar{v}$, respectively, being the charge, mass, and velocity of the electron. The magnetic field $\bar{B}$ is analytically calculated by introducing magnetic charges.[5,6] For calculating the electric field $\bar{E}$ it is assumed that $\bar{E}$ varies linearly within a distance d_E above the target surface, i.e., the potential $V(z)$ is given by

$$V(z)=\begin{cases}\dfrac{V_d}{d_E^2}[z-(z_0+d_E)]^2 & z_0+d_E\geqslant z\geqslant z_0\\ 0 & z>z_0+d_E\end{cases}. \tag{3}$$

Hence, d_E represents the sheath thickness. The Lorentz equation is numerically solved using the fourth order Runge–Kutta method.

For a position x_i the maximum height $z_{\mathrm{SE},i}$ that the SE can reach is deduced from the collisionless SE orbit. By retracing the magnetic field line that intersects the target at that position x_i the height $z_{\mathrm{MF},i}$ of the magnetic field line above the target at $x=0$ is determined. The z-value z_i of the center of arch A_i at $x=0$ is defined as

$$z_i=\frac{z_{\mathrm{SE},i}-z_{\mathrm{MF},i}}{2}. \tag{4}$$

The center line of the arch is defined by the magnetic field line going through z_i. We assume a homogenous spatial HEE distribution along this center line. According to Ref. 4 this is valid above the cathode sheath. In the following paragraph we deduce the correction factors needed within the sheath.

For the HEE only the interactions with neutral discharge gas atoms are taken into account as they are by far the most important.[7] Due to these interactions, the arches A_i contain HEE with energies ranging from $|eV_d|$ to $E_{\mathrm{ion,th}}$. We refer to this energy distribution of the HEE as $D(E)$. According to Ref. 8, $D(E)$ is practically homogenous. Because of this energy distribution, the homogenous spatial HEE distribution along the center line of the arch needs to be corrected within the cathode sheath. Indeed, at a position z in the sheath a HEE has a potential energy equal to $|eV(z)|$. Hence, only the HEE with energy higher than $|eV(z)|$ can reach that height z. As $D(E)$ is homogenous, the number $N(|eV(z)|)$ of HEE with energy higher than $|eV(z)|$ in the discharge is given by

$$N(|eV(z)|)=\int_{|eV(z)|}^{|eV_d|}D(E)dE\sim|eV_d|-|eV(z)|. \tag{5}$$

Similarly, the total amount of HEE is $N(E_{\mathrm{ion,th}})\sim|eV_d|$ because $|eV_d|\geqslant E_{\mathrm{ion,th}}$. Hence, the correction factor at height z in the sheath is $|eV_d\text{-}eV(z)|/|eV_d|$. In this way, the normalized spatial HEE distribution along the center line of each arch is determined.

The maximum distance a HEE can be away from the magnetic field line around which it gyrates is given by its Larmor radius r_L. As the gaussian distribution becomes practically zero at three times its width σ, we attribute to each arch A_i a gaussian distribution in the direction perpendicular to the magnetic field line. At $x=0$ this gaussian is represented by $G_i(z)$. Its width σ is set equal to $r_L/3$ and $G_i(z)$ reaches its maximum at the center z_i of the arch A_i (Fig. 2).

Downloaded 27 Dec 2012 to 152.14.136.96. Redistribution subject to AVS license or copyright; see http://avspublications.org/jvsta/about/rights_and_permissions

B. Modeling of the transfer of HEE among arches

A change in the direction of the velocity vector of a HEE due to an interaction with the discharge gas can transfer it from one arch (A_j) to another (A_i). The probability t_{ij} that this transfer occurs is proportional with the value of G_j around z_i. This is shown in Fig. 2 by the hatched surface at z_i. Introducing δz_i as $(z_{i+1}-z_{i-1})/2$ and linearizing G_j in the interval $[z_i-\delta z_i/2, z_i+\delta z_i/2]$ we find

$$t_{ij}\sim\int_{z_i-\frac{\delta z_i}{2}}^{z_i+\frac{\delta z_i}{2}} G_j(z)dz \approx G_j(z_i)\delta z_i. \tag{6}$$

From Fig. 2 it can be deduced that only the fraction $|x_i|/|x_j|$ of the arch A_j overlaps with A_i. Such partial overlap only occurs if $\Delta z_{ij}\leqslant\Delta x_{ij}$ with $\Delta x_{ij}=|x_i|-|x_j|$ and $\Delta z_{ij}=|z_i-z_j|$. As it reduces the transfer of HEE from A_j to A_i this interaction needs to be corrected with c_{ij}:

$$c_{ij}=\begin{cases}\dfrac{\Delta z_{ij}}{\Delta x_{ij}}+\left(1-\dfrac{\Delta z_{ij}}{\Delta x_{ij}}\right)\left|\dfrac{x_i}{x_j}\right| & \dfrac{\Delta z_{ij}}{\Delta x_{ij}}\leqslant 1\\ 1 & \dfrac{\Delta z_{ij}}{\Delta x_{ij}}>1\end{cases}. \tag{7}$$

Combining Eqs. (6) and (7) we find

$$t_{ij}\sim c_{ij}G_j(z_i)\delta z_i \tag{8}$$

from which the probabilities t_{ij} can be deduced by requiring

$$\sum_j t_{ij}=1. \tag{9}$$

This way the matrix T, which is a square matrix, is constructed. In reality the HEE do not interact once but several times. The probability t_{ij}^2 that at the second interaction the HEE transfers from A_j to A_i is given by

$$t_{ij}^2=\sum_k t_{ik}t_{kj}. \tag{10}$$

This is equal to element i,j of the matrix $T^2=T*T$. Hence, the element that gives the probability that a HEE that started in A_j is transferred to A_i at interaction m is element i,j of T^m. The accurateness of this approach is discussed in Sec. III.

C. Deduction of the HEE-density H

In this part we will deduce the relation between an emission profile r (a set of values r_i each of which corresponds with the amount of SE emitted at position x_i on the target) and the corresponding occupation profile u that characterizes the HEE distribution H in the discharge.

First, we take into account that only a fraction f_i of the SE released at x_i will effectively interact with the discharge gas because the rest is recaptured by the target. This recapture is due to the small initial energy of the SE when they are emitted from the target and is characterized by[5]

$$f_i=1-e^{-\frac{s_i}{\lambda}} \tag{11}$$

with s_i the average distance a SE emitted at x_i travels before it is recaptured and λ the mean free path of the SE in the discharge taking into account ionization, excitation, and elastic collisions. Hence, we can formulate an intermediate occupation profile u_i'':

$$u_i''=r_if_i. \tag{12}$$

Second, the creation of an electron-ion pair can produce a HEE if the ionization occurs at a height z for which $|eV(z)|>E_{\mathrm{ion,th}}$ is valid. When this happens, there is an extra energy input to the discharge equal to $|eV(z)|$ if the energy of the primary electron is not considered. This extra energy input by a HEE at height z can be described by giving the HEE a correction factor

$$1+\frac{|eV(z)|}{|eV_d|}. \tag{13}$$

For an arch A_i with $A_i(z)$ elements at height z the correction factor h_i is given by the weighted average of the individual correction factors

$$h_i=1+\frac{1}{|eV_d|}\frac{\sum_z |eV(z)|A_i(z)}{\sum_z A_i(z)}. \tag{14}$$

As deduced in the previous section a SE emitted in arch A_i has a probability T_{ji}^k to transfer to A_j at interaction k. Hence, due to ionization in the sheath, a SE emitted at position x_i needs a correction factor g_i given by

$$g_i=\prod_k\left(\sum_j h_jT_{ji}^k\right). \tag{15}$$

Thus, taking into account ionization in the sheath transforms u_i'' into u_i':

$$u_i'=u_i''g_i. \tag{16}$$

Third, we need the transfer matrix T_{avg} that describes the transfer of HEE among the arches averaged over $D(E)$. As $D(E)$ is constant, T_{avg} is given by

$$T_{\mathrm{avg}}=\frac{1}{n}\sum_{i=0}^{n-1}T^i, \tag{17}$$

because T^i contains the transfer probabilities at interaction i (T^0 represents the unit matrix). The number n represents the total amount of interactions a HEE undergoes until it has an energy below the ionization threshold $E_{\mathrm{ion,th}}$ (see also Sec. III). The final occupation profile u is then given by

$$u_i=\sum_k T_{\mathrm{avg},ik}u_k'. \tag{18}$$

Given Eq. (1) these u_i characterize the HEE distribution of the discharge.

D. Deduction of ionization and resulting target bombardment

For this part of the model we start from a known HEE distribution H. In order to deduce the ionization caused by this H we would in principle need to calculate the probability

Downloaded 27 Dec 2012 to 152.14.136.96. Redistribution subject to AVS license or copyright; see http://avspublications.org/jvsta/about/rights_and_permissions

$P(E)$ for an ionizing collision during a certain time interval ε_t for each electron energy E. The ionization probability $P(E)$ is given by

$$P(E)=1-e^{-\frac{\varepsilon_t v}{\lambda_{\mathrm{ion}}(E)}}=1-e^{-\frac{\varepsilon_t}{\lambda_{\mathrm{ion}}(E)}\sqrt{\frac{2E}{m}}}, \tag{19}$$

with $\lambda_{\mathrm{ion}}(E)$ as the electron mean free path for ionization. For E above approximately 100 eV, $\lambda_{\mathrm{ion}}(E)$ has an energy dependence close to $E^{0.5}$. Therefore, we consider $P(E)$ as independent of E which means $I \sim H$. Although the exact relation can be determined, this proportionality is sufficient as we limit ourselves to normalized distributions.

If we assume that the ions reach the target without undergoing any collisions,[9] the amount $Y_{\mathrm{SP},i}$ of sputtered target atoms at position x_i is calculated as

$$Y_{\mathrm{SP},i}=\sum_z I(x,z)y_{\mathrm{SP}}(|eV_d-eV(z)|), \tag{20}$$

with $y_{\mathrm{SP}}(E)$ as the ion energy dependent sputter yield. From this the erosion profile w can be determined as $w_i \sim -Y_{\mathrm{SP},i}$. For our calculations we used data for argon on aluminum.[10] Given the SE yield γ, we can deduce $Y_{\mathrm{SE},i}$ which is the amount of SE emitted from the target at position x_i:

$$Y_{\mathrm{SE},i}=\sum_z I(x,z)\gamma. \tag{21}$$

E. Self-consistency

The model so far allows to determine the normalized ionization distribution I for a given emission profile $r_{i,0}$. This I leads to the SE emission profile $Y_{\mathrm{SE},i}$ at the target which is in fact a new emission profile $r_{i,1}$. In steady state (SS) both emission profiles should be the same. To find this SS emission profile $r_{i,\mathrm{SS}}$ the procedure that leads from $r_{i,0}$ to $r_{i,1}$ is repeated, each time redefining $r_{i,1}$ as the new $r_{i,0}$. Through iteration the ratio $r_{i,1}/r_{i,0}$ can be made constant for a given magnet system, discharge voltage V_d, sheath region d_E, and pressure p. However, the condition $r_{i,1}=r_{i,0}=r_{i,\mathrm{SS}}$ can only be obtained for a particular pressure (Sec. IV). Therefore, when a constant $r_{i,1}/r_{i,0}$ was reached the pressure was varied until $r_{i,0}=r_{i,1}=r_{i,SS}$ was found. Then, I was integrated over the x direction so that the normalized ionization profile in the direction perpendicular to the target was obtained. The position z_M of the maximum of this profile was determined. According to simulations of Kondo and Nanbu[11] the distance above the target where the ionization density is the highest (z_M) is approximately equal to the distance above the target where the electric field becomes practically zero (d_E). Consequently, the whole procedure was iterated until d_E equal to z_M was obtained. Therefore, we can conclude that through iteration a self-consistent SE emission profile, pressure, and cathode sheath thickness is obtained for a given magnet system and discharge voltage.

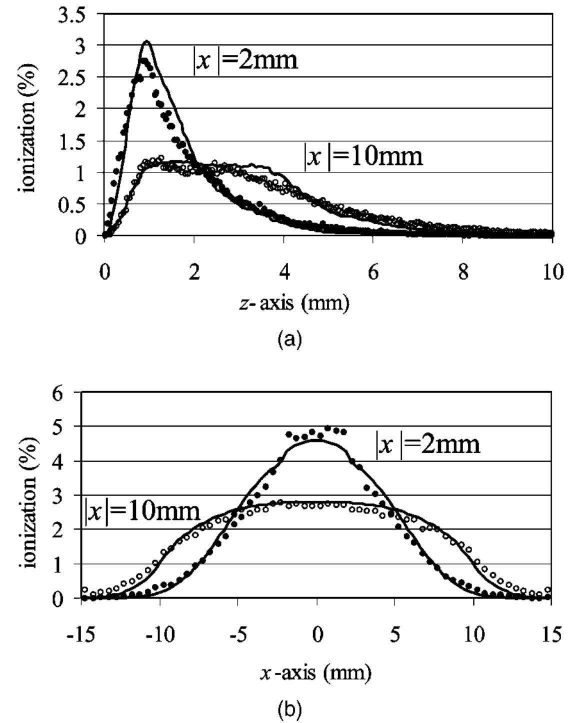

FIG. 3. Plots of the normalized ionization distributions I (solid line) and I_{MC} (dots) integrated along the x axis (a) and along the z axis (b) for $|x|=2$ and $|x|=10$ mm. The magnet system used for these calculations is defined by $d=36$ mm, $s=12$ mm, $B_r=0.7$ T and $z_0=15$ mm. Furthermore we set $V_d=-300$ V and $p=0.5$ Pa.

III. COMPARISON WITH MC SIMULATIONS

In Sec. II several assumptions were made to model the motion of the HEE and their interactions. Therefore, results from our model are compared with MC results. We use the geometry shown in Fig. 1 with a magnet system described by $d=36$ mm, $B_r=0.7$ T, and $s=12$ mm. This results in a maximum horizontal magnetic field strength at the target surface of 0.061 T. Furthermore, we choose $V_d=-300$ V and $z_0=15$ mm. In this section the sheath thickness d_E and the pressure p are assumed to be known and given the values 1.0 mm and 0.5 Pa, respectively. The Lorentz equation [Eq. (2)] for the electron motion is combined with the algorithm found in Ref. 12 for MC treatment of the collisions. Ionization, excitation, and elastic collisions were taken into account by using the cross sections as reported by Kosaki and Kondo.[13] Only energy loss due to ionization and excitation is considered: for an ionization the electron energy reduction was approximated by 16 eV ($=E_{\mathrm{ion}}$), for an excitation by 12 eV ($=E_{\mathrm{exc}}$).[5] From the positions $x=-10$, -2, 2 and 10 mm 2000 electrons were emitted and followed until a limit of 2 μs had elapsed or until their energy dropped below 30 eV, whichever occurred first. This energy threshold was chosen because below this energy the probability for an ionization is very small. In this way the ionization distribution I_{MC} in the xz plane is determined. The integrated profiles along the x axis and z axis of I_{MC} are shown in Fig. 3 for $|x|=2$ and $|x|=10$.

Downloaded 27 Dec 2012 to 152.14.136.96. Redistribution subject to AVS license or copyright; see http://avspublications.org/jvsta/about/rights_and_permissions

These simulations reveal that on average approximately 30% of the collisions were ionizing, 10% were excitations and 60% were elastic collisions. This means that in this electron energy range the total number of collisions n which an electron undergoes (needed for Sec. II) can be approximated by three times the number of ionizing collisions n_{ion}. The number n_{ion} is given by:

$$n_{\text{ion}}=\frac{E-E_{\text{ion,th}}}{E_{\text{ion,eff}}}, \tag{22}$$

with $E_{\text{ion,eff}}$ the average effective energy needed to create an ion-electron pair. Taking into account only ionizations and excitations as energy dissipating collisions, $E_{\text{ion,eff}}$ is determined by

$$E_{\text{ion,eff}}=\frac{n_{\text{ion}}E_{\text{ion}}+n_{\text{exc}}E_{\text{exc}}}{n_{\text{ion}}}. \tag{23}$$

Given the relative occurrence of ionization and excitation we find $E_{\text{ion,eff}}\approx 20$ eV which is lower than the value of 30 eV proposed by Thornton.[14] Based on these MC results we approximate n for a discharge with V_d as

$$n\approx 3\frac{|eV_d|-16}{20}. \tag{24}$$

To compare the MC results with our model we define the following emission profile r:

$$r_i=\begin{cases}0 & |x_i|\neq 2\\ 1 & |x_i|=2\end{cases}. \tag{25}$$

As n is known, Eqs. (1) and (12)–(18) allow to determine I corresponding with an electron emitted at $|x|=2$. The integrated profiles along the x axis and z axis of I are shown in Fig. 3 for $|x|=2$. Similarly, the I corresponding with $|x|=10$ can be determined. As can be seen agree I and I_{MC} very well for both x positions which shows the validity of our approach. Moreover, the proposed method calculates the ionization distribution practically instantaneously compared with the MC simulations.

IV. RESULTS AND DISCUSSION

A. Discharge properties for a given V_d and magnet system

For the calculations in this section the same magnet system as in Sec. III is used. To determine the properties of the arches, SE were released from the target at positions $x=0.125,0.375,...,14.875$. For calculating the recapture probabilities the SE were given an initial energy equal to 4 eV. The discharge voltage was set to -300 V, a typical value for a laboratory scale planar magnetron. To start the iteration procedure d_E was set to 1.0 mm and p to 0.5 Pa. In the SS we found $p=0.26$ Pa and $d_E=0.97$ mm. The corresponding emission profile r_{SS} that gives the relative amount of SE emitted at the target is plotted in Fig. 4. Due to interactions, the original emission profile evolves into the occupation profile u_{SS}. Comparing r_{SS} and u_{SS} reveals that although most SE are emitted at the center of the race track (here $x=0$) the

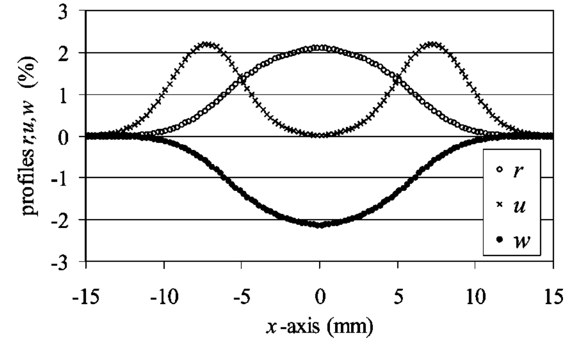

FIG. 4. Steady state results of the emission profile r, the occupation profile u and the erosion profile w along the target for a discharge with the same magnet system as used for Fig. 3. V_d was set to -300 V. The self-consistent pressure of this system is 0.26 Pa.

most occupied arches have larger absolute x values (here $5<|x|<10$). The erosion profile w_{SS} corresponding with the occupation profile u_{SS} is also plotted in Fig. 4.

For a given V_d and magnet system the iteration procedure results only for a particular pressure in a SS solution (Sec. II). In order to understand this we recall the equation for determining the minimum discharge voltage $V_{d,\min}$ in a planar magnetron[15]

$$|eV_{d,\min}|=\frac{E_{\text{ion,eff}}}{\gamma_{\text{eff}}}, \tag{26}$$

with γ_{eff} as the effective SE yield as seen by the discharge. In Ref. 15 $\gamma_{\text{eff}}=0.5\gamma$ is assumed which is based on an estimation of Thornton.[14] Starting from an emission profile r_{SS} we are able to calculate γ_{eff}: from Eqs. (12) and (16) follows that r_i emitted SE result in $r_i f_i g_i$ HEE in the discharge. Hence, a position x_i has an effective SE yield $\gamma_{\text{eff},i}$ given by

$$\gamma_{\text{eff},i}=\gamma f_i g_i. \tag{27}$$

The effective SE yield as seen by the discharge is then the r_i weighted average of $\gamma_{\text{eff},i}$:

$$\gamma_{\text{eff}}=\frac{\sum_i \gamma_{\text{eff},i}r_i}{\sum_i r_i}=\gamma\frac{\sum_i f_i g_i r_i}{\sum_i r_i}. \tag{28}$$

We find for the SS solution $\gamma_{\text{eff}}=0.067$ which results in $V_{d,\min}=V_d$. Hence, the pressure found through the iteration procedure is the pressure for which V_d is the theoretical minimum discharge voltage $V_{d,\min}$.

B. Pressure dependence of the discharge

For a whole range of V_d the SS condition and corresponding discharge properties were simulated. Based on these results $V_{d,\min}$ is plotted as a function of pressure in Fig. 5(a): at high pressures $V_{d,\min}$ varies only slowly with pressure while at low pressures it increases strongly with decreasing pressure. This pressure dependence corresponds well with the observations reported by Chang *et al.*[16] However, they measured that at high pressures the discharge voltage remains almost constant while our simulations show a slight decrease. This is probably because of the assumption of collisionless ion movement in our model which is no longer valid

Downloaded 27 Dec 2012 to 152.14.136.96. Redistribution subject to AVS license or copyright; see http://avspublications.org/jvsta/about/rights_and_permissions

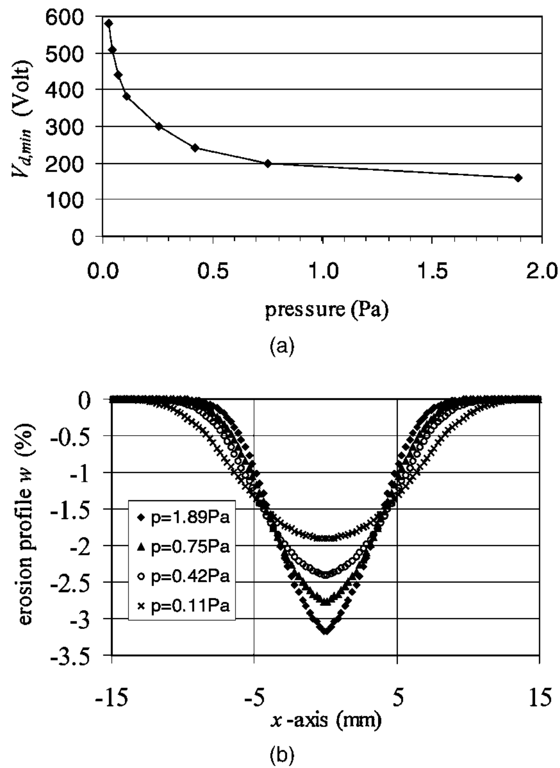

FIG. 5. The pressure dependence of $V_{d,\min}$ (a) and of the erosion profile w (b) for the same magnet system as Fig. 3.

at these high pressures. In Fig. 5(b) the normalized erosion profiles for four different pressures are plotted: at high pressures the pressure dependence is weak but it becomes stronger with decreasing pressure. We reported the experimental observation of this widening of the erosion profile in previous work.[5] These simulation results confirm the explanation given for the widening of the erosion profile: with decreasing pressure (increasing λ) the fraction f_i of SE that effectively interacts with the discharge decreases [Eq. (11)]. This effect is stronger for SE emitted at small absolute x (inner arches) as for SE emitted at large absolute x (outer arches).[5] Hence, with decreasing pressure, u_i of the outer arches becomes larger. Figure 3(b) shows that the ionization caused by the outer arches (represented by $|x|=10$ mm) is spatially more spread than the ionization caused by the inner arches (represented by $|x|=2$ mm). Consequently, with decreasing pressure the erosion profile widens. Fig. 4 shows that at 0.26 Pa the outermost arch is hardly occupied. This remains valid even at the lowest pressures for the simulated magnet system. Hence, the increase of V_d is not due to the increased escape of electrons out of the magnetic trap with decreasing pressure. Instead, it is due to the increased recapture of SE: Eq. (28) shows that the reduced f_i results in a smaller γ_{eff}. Hence, according to Eq. (26) the discharge voltage has to raise. The importance of recapture shows that it is necessary to take into account the initial energy of the SE when they are emitted from the target as it is this small energy that determines recapture (Sec. II C). As the simulation procedure was performed using a "typical" magnet system in comparison with the experiment, exact quantitative agreement cannot be expected. Nevertheless, the good qualitative agreement between experiments and simulations for the pressure dependence of both discharge voltage and erosion profile and the realistic values found for the self-consistent pressures show the validity of the model.

V. CONCLUSIONS

In this article we presented a two-dimensional model for a planar magnetron discharge. The model is based on the motion of the HEE which are the electrons with enough energy to ionize. For sufficiently strong magnetic fields this motion can be modeled by considering the discharge as built up by arch shaped regions. The properties of the arches were determined by calculating the collisionless secondary electron orbits corresponding with these arches. The interactions of the HEE with the discharge gas are modeled by introducing interaction matrices that describe the transfer of HEE among the arches. From the HEE distribution the ionization can be deduced. There is good agreement between this method and Monte Carlo simulations.

Once the ionization is known, the SE emission and the sputter erosion can be calculated. For a given magnet system and discharge voltage the cathode sheath thickness can be determined through iteration. It appeared that this was only possible for a specific pressure, namely the pressure for which the discharge voltage is the theoretical minimum discharge voltage to maintain the discharge. The model was able to reproduce the experimentally reported pressure dependence of the discharge voltage and erosion profile of a planar magnetron. Moreover, the model reveals that the main cause for the pressure dependence is not the escape of electrons out of the magnetic trap but the recapture of SE at the target.

ACKNOWLEDGMENT

This research is financed with a grant from the Institute for the Promotion of Innovation by Science and Technology in Flanders (IWT).

[1]C. H. Shon and J. K. Lee, Appl. Surf. Sci. **192**, 258 (2002).
[2]A. V. Phelps and Z. Lj. Petrović, Plasma Sources Sci. Technol. **8**, R21 (1999).
[3]S. Ido, Y. Ishida, and K. Hijikata, Jpn. J. Appl. Phys., Part 1 **32**, 2112 (1993).
[4]A. E. Wendt, M. A. Lieberman, and H. Meuth, J. Vac. Sci. Technol. A **6**, 1827 (1988).
[5]G. Buyle, D. Depla, K. Eufinger, J. Haemers, W. De Bosscher, and R. De Gryse, 45th SVC Annual Technical Conference Proceedings ISSN 0737-5921 (2002), p. 348.
[6]W. Andrä, B. Danan, and R. Mattheis, Phys. Status Solidi A **125**, 9 (1991).
[7]T. E. Sheridan, M. J. Goeckner, and J. Goree, J. Vac. Sci. Technol. A **8**, 30 (1990).
[8]F. Guimarães, J. Almeida, and J. Bretagne, J. Vac. Sci. Technol. A **9**, 133 (1991).
[9]K. Okazawa, E. Shidoji, and T. Makabe, J. Appl. Phys. **86**, 2984 (1999).
[10]S. M. Rossnagel, IBM J. Res. Dev. **43**, 163 (1999).
[11]S. Kondo and K. Nanbu, J. Phys. D **32**, 1142 (1999).

Downloaded 27 Dec 2012 to 152.14.136.96. Redistribution subject to AVS license or copyright; see http://avspublications.org/jvsta/about/rights_and_permissions

[12]A. Bogaerts, Ph.D. Thesis, Universiteit Antwerpen, 1996.
[13]K. Kosaki and M. Hayashi, Preprint Natl. Meeting Ins. Electr. Engr., Jpn. (in Japanese) (1992). See S. Kondo and K. Nanbu, Rep. Inst. Fluid Sci. **12**, 101 (2000). A tabulation of these cross sections is available at ftp://jila.Colorado.edu/collision_data/electronneutral/hayashi.txt.
[14]J. A. Thornton, J. Vac. Sci. Technol. **15**, 171 (1978).
[15]M. A. Lieberman and A. J. Lichtenberg, *Principles of Plasma Discharges and Materials Processing* Wiley, New York, 1994), p. 468.
[16]S. A. Chang, M. B. Skolnik, and C. A. Altman, J. Vac. Sci. Technol. A **4**, 413 (1986).

Downloaded 27 Dec 2012 to 152.14.136.96. Redistribution subject to AVS license or copyright; see http://avspublications.org/jvsta/about/rights_and_permissions